Effect of double thermal and electrochemical oxidation on titanium alloys for medical applications

Agnieszka Ossowska, Jean-Marc Olive, Andrzej Zieliński, Andrzej Wojtowicz

Applied Surface Science 563 (2021) 150340

Contents lists available at ScienceDirect

Applied Surface Science

journal homepage: www.elsevier.com/locate/apsusc

Full Length Article

Effect of double thermal and electrochemical oxidation on titanium alloys for medical applications

Agnieszka Ossowska [a,*], Jean-Marc Olive [b], Andrzej Zieliński [a], Andrzej Wojtowicz [c]

[a] Gdansk University of Technology, Faculty of Mechanical Engineering and Ship Technology, 11/12 Narutowicza St., 80-233 Gdańsk, Poland
[b] Institut de Mécanique et d'Ingénierie, Université de Bordeaux, 33405 Talence CEDEX, France
[c] Medical University of Warsaw, Department of Dental Surgery, Warsaw, Poland

ARTICLE INFO

Keywords:
Titanium alloys
Thermal oxidation
Electrochemical oxidation
Coatings
Microstructure
Nanoindentation
Cytotoxicity
Antibacterial efficiency

ABSTRACT

The research focuses on the development and characterization of innovative thin hybrid oxide coatings obtained in subsequent processes of thermal (TO) and electrochemical (EO) oxidation. Four different surface modifications were investigated and the microstructure was determined, the mechanical, chemical and biological properties of the Ti-13Nb-13Zr alloy were assessed using scanning electron microscopy, X-ray dispersion analysis, glow discharge emission spectroscopy, Raman spectroscopy, nanoindentation and corrosion resistance measurements. The composite layers were evaluated for antimicrobial activity, cytotoxicity bioassays and wettability tests were performed. The conducted studies of two-stage oxidation (TO + EO) have shown that it is possible to obtain layers with a different structure - crystalline and nanotubular. The formation of a nanotube layer on the surface of the crystalline layer is dependent on the thickness of the crystalline layer. The produced double titanium oxide coatings show high surface roughness, high corrosion resistance, are hydrophilic, slightly antibacterial, and not cytotoxic, which has a huge impact on the process of connecting the tissue with the implant.

1. Introduction

Titanium and its alloys are widely used for materials implanted into the human body. Despite their very good properties such as fatigue strength [1] and corrosion resistance [2–5], and low Young's modulus [6,7], they cannot provide long-term service life. In the first days after implantation, they are not able to establish a connection with human tissue as they are bioinert. The natural layer, a spontaneously forming compact and homogeneous passive oxide layer on titanium (1.5–10 nm), insufficiently protects the implant against corrosion in physiological fluids. Besides, natural titanium oxide has low bioactivity and shows weak binding to bone tissue [8] due to a grown layer of soft tissue (fibrosis) preventing direct contact of the implant surface with the bone [9,10]. Fibrosis is a natural process that leads to vascularization [11] and the formation of fibrocartilage, followed by the formation of bone tissue [12–14], and it is not prevented by a natural oxide layer. To improve the surface properties, increase bioactivity, and resistance to the corrosive effects of the biological environment, titanium alloys are subjected to different modifications, which consist of one or more surface treatments. Thanks to the surface modification of titanium alloys [15–28] used in implantology, it is possible to improve the mechanical binding between implant and bone by increasing the bioactivity of the implant and decreasing the healing time by accelerating the processes of osseointegration [9,29–34]. Modifications of the implant surface are sought to particularly increase the biocompatibility and bioactivity, corrosion resistance, and service life of the implants [35].

Recent research on metallic biomaterials has been focused on the issues related to the thin surface engineering of implants, the formation of the top layers involving a base metal, and ceramic or composite coatings which show favorable physical, chemical, and mechanical properties [36] and allow controllable reactivity, minimize post-operative complications and, consequently, enable the faster return of the patient to full mobility.

Thermal oxidation (TO) is one of the simplest techniques of surface modification, allowing the improvement of titanium properties by creating oxide layers [37–39]. It is a promising way to protect metals and alloys from the negative impact of the environment by the formation of protective coatings on their surface [40–42]. Thermal oxidation takes place under the influence of dry gases without the use of an electrolyte. It is carried out at high temperatures ranged from 400 °C to 1100 °C [43–46]. The process of titanium oxidation is characterized by the simultaneous dissolution of oxygen in the metallic phase and the

* Corresponding author.
E-mail address: agnieszka.osssowska@pg.edu.pl (A. Ossowska).

https://doi.org/10.1016/j.apsusc.2021.150340
Received 6 April 2021; Received in revised form 30 May 2021; Accepted 8 June 2021
Available online 12 June 2021

formation of solid oxidation products in the form of scale [47]. As a result of TO, the stress increases in the layer, and when reaching a critical value, it leads to the formation of gaps and cracks on the surface [48]. The created layers form a stable and adhesive ceramic oxide (TiO_2) coating, which can be found in several crystallographic forms such as rutile, anatase, and brucite [49]. The obtained oxide coatings improve the corrosion and wear resistance, and biocompatibility [43–45]. The properties of the oxide layer depend on the oxidation kinetics [50,51].

A different technique for obtaining oxide layers is electrochemical oxidation, a technique allowing appropriate selection of parameters and resulting in oxide layers of various structures and thicknesses, including nanostructures with bioactive and osteoconductive properties [52,53]. Nanotubular layers are used in medicine for several reasons. First of all, TiO_2 nanotube layers formed on the implant surface show biocompatibility, significantly improve hydrophilicity, adhesion, and proliferation of osteoblasts, and promote osseointegration [54,55]. The nanotubes create a surface topography similar to that of natural bone tissue while increasing the surface roughness in the nanoscale. The quality and geometric shape of the substrate determine the behavior of cells and their adhesion to the substrate [56]. It is known that osteoblasts (bone-forming cells) tend to adhere to rough surfaces, morphologically and chemically similar to natural bone tissue [57,58]. In contrast, fibroblasts (connective tissue cells) prefer smooth surfaces [59]. The adhesion, proliferation, and migration of the cells that make up the bone tissue are related to the diameter of the nanotubes. Bauer et al. [60] found that nanotubes with a diameter of about 15 nm were more stimulating for cell growth and differentiation while for those with diameters of about 100 nm, a drastic increase in cellular apoptosis (death) could appear. However, there is still no clear answer as to the optimal diameter of the nanotubes that would stimulate cell growth and differentiation. Titanium oxide nanotubes, despite their attractive biological and physicochemical properties, are characterized by low mechanical parameters, especially they are prone to brittle fracture [61].

In this research, new duplex oxide coatings (which may be also called sandwich, hybrid, or bi-layer coatings) were produced by two-stage oxidation. The inner layer was designed to increase corrosion resistance and therefore also biocompatibility and long-lasting the implant. The outer layer was conceived as a nanotubular layer leading to the bioactivity of the implant. The first inner layer was obtained by thermal oxidation while the second layer by electrochemical oxidation. As a result of such a surface modification process, an improvement in the mechanical and chemical properties of the material was expected in particular.

2. Materials and methods

2.1. Materials

The research was carried out on Ti-13Nb-13Zr titanium alloy manufactured by SeaBird Metal Materials Co., China. This two-phase alloy had the β-phase and α' phase, and martensitic structure. The chemical composition of the alloy was: Nb 13.5; Zr 13.5; Fe 0.05; C 0.04; N 0.013; H 0.004; O 0.11 mass pct., and Ti as the remainder.

Alloy sheet was cut into specimens of dimensions 15x10x4.2 mm. The samples were then grounded with abrasive paper No. 2500 as the last (Struers Inc., USA). Finally, the samples were cleaned in an ultrasonic chamber (Sonic-2, Polsonic Palczynski, Warsaw, Poland) for 5 min in, subsequently, distilled water, methanol, and isopropanol (chemicals supplied by Avantor Performance Materials Poland S.A., Gliwice, Poland) and dried in laboratory air.

2.2. Thermal and electrochemical oxidation

The coatings were prepared by a two-step procedure using two subsequent oxidation methods. In detail, the thermal oxidation process was performed to achieve the continuous inner oxide layer (TO), and then the nanotubes were produced on such surface by the electrochemical method (EO).

The thermal oxidation process was conducted in an air atmosphere, at temperatures 700, 800, and 900 °C for 4 h. The specimens were thermally treated in a tubular furnace (Protherm PC442, Ankara, Turkey), heated at a rate of 3 °C/min, and cooled to room temperature in the furnace.

The electrochemical oxidation was performed in a standard electrical circuit composed of a power supply (SPN-110-1C, MPC Lab Electronics, Netherlands), the tested titanium sample as an anode, and the Pt electrode as a cathode. All measurements were performed at a potential of 20 V for 30 min at room temperature (parameters already used in [62] in neither stirred, aerated nor deaerated solution. The anodization parameters were set up based on some earlier investigations [62]. The oxidation started after 30 min from the immersion of a sample in solution to reach a steady-state condition. After any process, the specimens were rinsed in deionized water and dried in laboratory air.

2.3. Structure and morphology

The samples' topography and cross-sections of all oxide layers were examined using the scanning electron microscope (SEM JEOL JSM-7600F, JEOL Ltd., Tokyo, Japan), equipped with an LED detector, at an acceleration voltage of 5 kV. The X-ray energy-dispersive spectrometer (EDS, Edax Inc., USA) was applied to determine surface chemical composition.

The roughness measurements were carried out by atomic force microscopy (Asylum Research MFP 3D, Oxford Instruments, USA) at the Universite Bordeaux, France. The surface topography was observed by the non-contact mode setting force of 50 mN. The roughness was calculated as an average of all measurements made in an area of 5.0x5.0 μm.

The phase studies were performed using the X-ray diffractometer (Philips X'Pert Pro –MPD, United Kingdom) with a vertical T-T goniometer (190 mm radius). The Cu -ray source was operated at 40 kV, 50 mA.

The spectroscopic examinations of obtained oxide layers using the Raman spectrometer (Jobin-Yvon, USA) were made at the Max Bergmann Centrum of Biomaterials, Dresden Technical University.

The glow discharge optical emission spectroscopy (GDOES) tests were done by the GD-Profiler 2 (Horiba Jobin Yvon, USA) at the Universite Bordeaux, Institut de Mecanique et des Materiaux, at 700 Pa of pressure, 30 W power, and 120 s measurement time.

2.4. Nanomechanical studies

The nanoindentation tests were carried out with nanoindenter (NanoTest Vantage, Micro Materials, United Kingdom) employing the Berkovich tip. The applied force was equal to 5 mN, the loading and unloading times were 20 s, and the dwell period under full load was 10 s. The subsequent indents were made at a distance of 50 μm. Oliver and Pharr method was applied to obtain the load–displacement curves. The reduced Young's modulus (E) and the surface hardness (H) were determined. The Poisson's ratio value of 0.3 was used to calculate Young's modulus. The mean values were achieved based on 5 independent tests each.

2.5. Contact angle studies

The measurements were done with a contact angle goniometer (Zeiss, Germany) by falling water droplet method, at room temperature. The mean values were calculated based on three independent attempts each.

2.6. Corrosion resistance research

The corrosion parameters were determined by a potentiodynamic method. The test Ringer's solution had composition: 2.25 g NaCl, 0.105 g KCl, 0.06 g $CaCl_2$, and 0.05 g $NaHCO_3$ in 1 L of water (Merck KGaA). The tests were performed at pH 7, 5, and 3; the lowest value was applied to simulate inflammation states [67]. The potentiostat/galvanostat (VersaSTAT 4, Ametek Scientific Instrumentation, UK) and an electrochemical cell composed of titanium anode, Pt cathode, and SCE (saturated calomel electrode) as reference electrode was used.

The samples were stabilized at their open circuit potential (OCP) for 0.5 h before the test. The potential was changed at a rate of 10 mV/min between −2 and 2.5 V. The corrosion potential E_{corr} and corrosion current density i_{corr} were found from the intercepts of polarization curves based on the Tafel extrapolation method.

2.7. Biological assessment of antibacterial activity

Studies of antibacterial activity of nanotubular surfaces were carried out at the Gdansk University of Technology, Faculty of Chemistry, with the *S. aureus* ATCC25923 strain. The samples were deposited in 5 mL of bacterial suspension (containing at least 10^6 colony forming units, CFU, in 1 cm^3) prepared in phosphate-buffered saline (PBS: 8.0 g NaCl, 0.24 g KH_2PO_4, 0.2 g KCl, 1.44 g Na_2HPO_4 in 1 L of distilled water), in which they remained for 1 min at room temperature. Then the samples with bacteria adsorbed on their surfaces were moved to 5 mL of sterile Trypticase Soy Broth (TSB) medium placed in the 8-well microplates. The samples were incubated at 37 °C for 24 h (one day) or 120 h (5 days). Subsequently, the samples were carefully removed from the TSB medium and rinsed by submersion, three times in 0.9% NaCl solution. Afterward, the samples were placed in the wells of a new titration plate containing 5 mL of MTT (3-(4,5-dimethyl-2-thiazolyl)-2,5-diphenyl-2*H*-tetrazolium bromide) solution (0.3%) in PBS. The living bacteria cells reduced MTT to insoluble in water violet formazan crystals (the amount of formed formazan is proportional to the number of live bacteria still present in the form of biofilm on the surface). Next, after 2 h incubation at 37 °C in the dark, the solution of MTT in PBS was carefully removed from the wells and replaced with 5 mL of dimethyl sulfoxide (DMSO) for dissolving formed formazan crystals. The optical density of the obtained solutions was measured at 540 nm using a Victor^3 microtiter reader (Perkin Elmer, Waltham, MA, USA).

2.8. Biological tests of cytotoxicity

Cytotoxicity tests were performed at the Warsaw Medical University, Department of Dental Surgery, on fibroblasts obtained from neonatal rat Lewis Op/Op after the third passage. A small microscope slide was placed into small plastic plates with a diameter of 35 mm (Corning, 430165). For each of them, except for control plates, single titanium samples were filled with a suspension of cells in the culture medium. All plates contained 100,000 cells suspended in a 2.0 mL of medium. After five days, the slides with the deposited cells were rinsed with physiological saline and preserved in a mixture of methanol and acetic acid (3:1) for 5 min, and then stained with hematoxylin and eosin. The preparations were dehydrated with DPX (a mix of distyrene, a plasticizer, and xylene), dried, and subjected to microscopic evaluation. The density of cultured cells and their morphological features, as well as the presence of forms of mitotic divisions, were assessed. The evaluation of each sample was carried out three times.

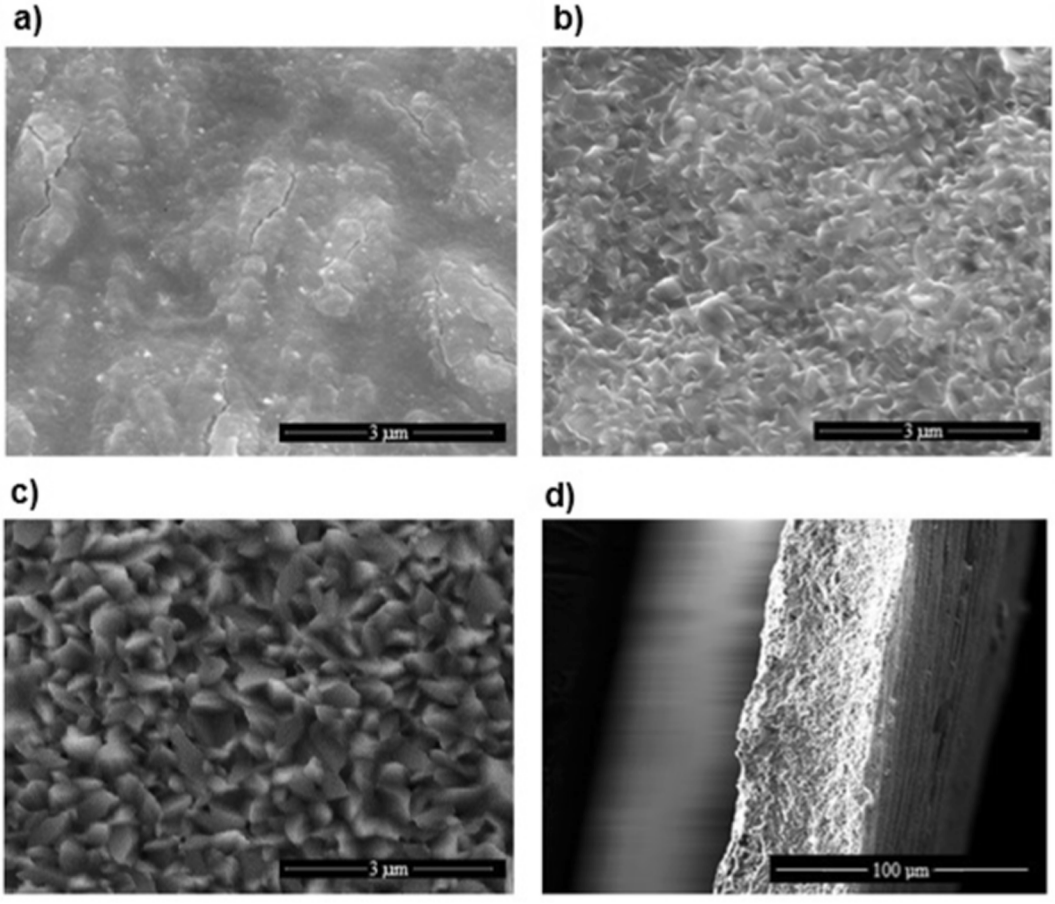

Fig. 1. The coating morphology after thermal oxidation: (a) 700 °C, (b) 800 °C, (c) 900 °C, (d) cross-section after thermal oxidation at 700 °C.

3. Results

3.1. Surface topography and thickness of coatings

Fig. 1 presents several images of the thermally prepared oxide coatings. The coatings differed in surface quality and layer thickness. The layers produced at the temperature of 700 °C were the thinnest (50–68 μm; Fig. 1d) and homogenous, however, they had single small cracks. As the temperature of the thermal oxidation process increased, the structures of the layers changed, and crystalline layers began to form, the volumes of individual crystals gradually increased. The thicknesses of the oxide layers increased with oxidation temperature, at 800 °C it was 78–87 μm, and at 900 °C, it was 90–97 μm.

After thermal oxidation was carried out, the next step was to create nanotubular layers with the use of electrochemical oxidation. The compact homogenous layers of nanotubes were obtained on the native material and thermally modified samples at the temperature of 700 °C (Fig. 2). On the surface of the remaining samples, subjected to oxidation at a higher temperature, no nanotube-like layers were observed.

The thickness of the EO nanotubular layer was about 1000 nm, but for the layer produced after previous heat oxidation (TO) thickness of the nanotube layer was lower than that formed on the polished titanium alloy Ti-13Nb-13Zr, with the same process parameters, being in the range of 725–773 nm (Fig. 2b, d). However, no differences in the diameters of the nanotubes between EO and TO + EO were observed, their sizes ranged from 40 nm to 120 nm. Also, the thickness of the nanotube walls was the same for EO and TO + EO, from 10 nm to 25 nm.

The formed layers had a different chemical composition (Table 1). The modification of the Ti-13Nb-13Zr alloy surface showed that the layer contained fewer alloying elements (Ti, Nb, Zr).

Lopes et al. [63] also observed a decrease in the share of Ti ions in the outer oxide layer formed on the TiNbZr alloy. This is most likely due to the slower diffusion of elements Ti and Nb, compared to the diffusion rate of Zr. This fact is consistent with the Ellingham diagram which

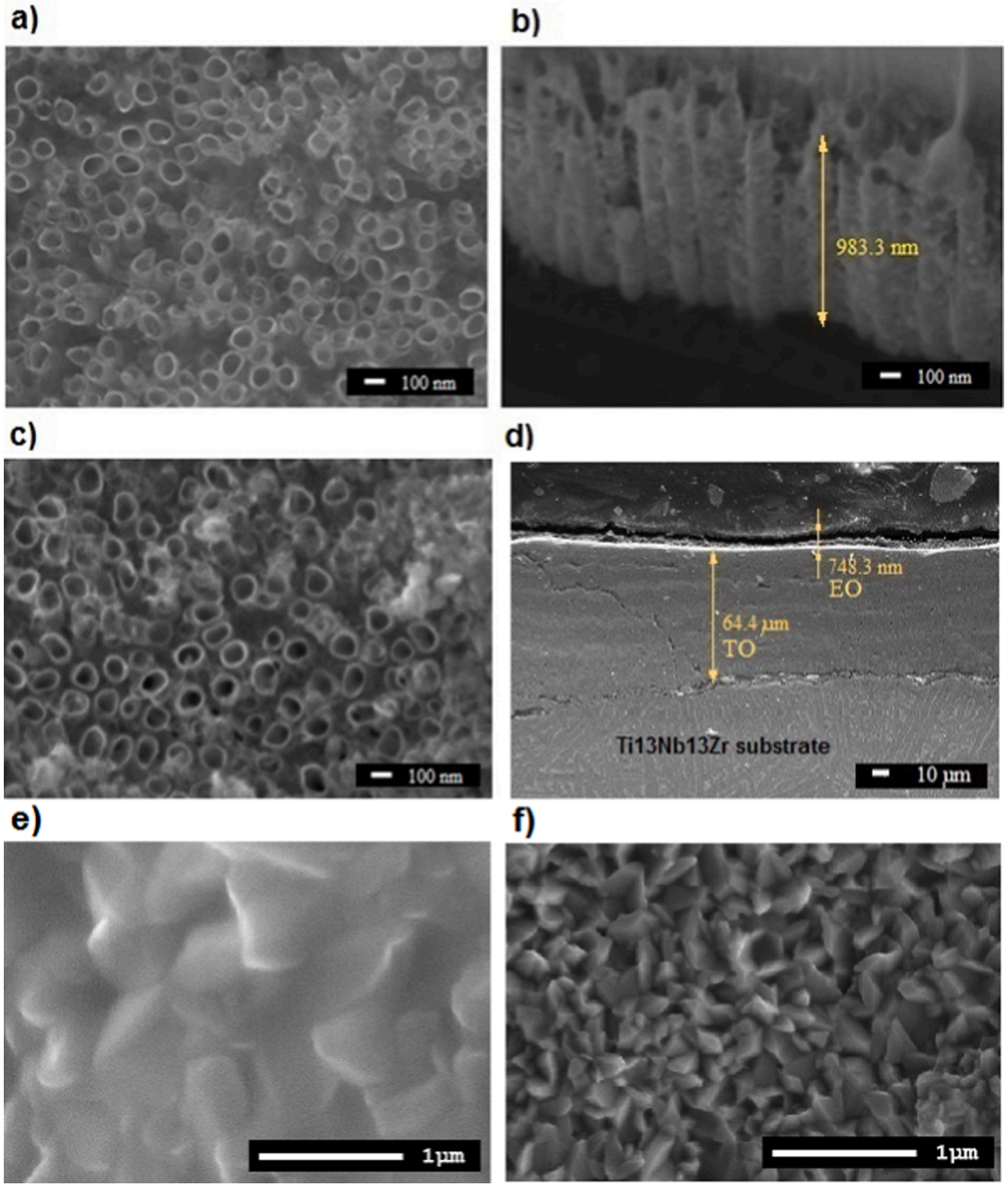

Fig. 2. The coatings morphology after electrochemical oxidation to the samples: (a) EO; (b) cross-section for EO; (c) TO (700 °C) + EO, (d) cross-section after TO (700 °C) + EO, (e) TO (800 °C) + EO, (f) TO (900 °C) + EO.

Table 1
EDS examinations of tested specimens.

Element	Ti-13Nb-13Zr	TO	EO	TO + EO
	Mass pct.	Mass pct.	Mass pct.	Mass pct.
O*	1.80 ± 0.79	46.86 ± 4.49	41.34 ± 5.09	58.83 ± 10.37
Ti	72.17 ± 5.15	39.72 ± 3.26	44.13 ± 4.92	25.30 ± 2.19
Nb	13.03 ± 0.41	6.65 ± 0.29	3.72 ± 0.16	5.13 ± 1.70
Zr	13.00 ± 0.40	6.77 ± 0.24	5.54 ± 2.36	5.50 ± 1.68
F	–	–	3.50 ± 2.87	3.43 ± 0.55
P	–	–	1.77 ± 0.98	1.81 ± 0.4

shows that the oxidation of Zr is faster compared to that of Nb [64]. On the other hand, Golvano [65] noticed that the passive layer formed on the Ti-13Nb-13Zr titanium alloy was a mixture of TiO_2, ZrO_2, and Nb_2O_5 oxides, unlike for other titanium alloys (e.g.: Ti5Al2.5Fe, Ti15Mo2.8Nb3Al, Ti15Mo5Zr3Al, Ti6Al4V), which could form uniform compact layers on the surface, comprising of TiO_2 and traces of other oxides.

With the increase of the thermal oxidation temperature, the mass fraction of oxygen in the layer increased, while the fraction of titanium decreased. The oxygen content in the layer was determined from the stoichiometry (hence the asterisk symbol for oxygen content). Based on EDS readings, the elementary content of each alloying metal was determined. Then, assuming that oxygen formed the appropriate stoichiometric oxides, the oxygen content was calculated and the whole was normalized to 100%. By examining the percentage composition of the elements niobium and zirconium in the titanium alloy (native material), subject only to grinding and polishing processes, it can be seen that both of these elements are in nominal percentage limits. As a result of oxidation, the mass fractions of all alloying elements decreases. The subtle differences are noticed among the chemical composition of the samples. It may be suggested that taking into account even the contaminants found after electrochemical oxidation, thermal oxidation results in the increasing fraction of oxides of Zr and Nb, likely due to faster diffusion of these elements at high temperatures.

The surface coating topography after different thermal and electrochemical oxidation is shown in Fig. 3, and Fig. 4 presents the roughness of coatings. For the native Ti-13Nb-13Zr titanium alloy, the lowest surface roughness was obtained thanks to polishing the surface. On the other hand, for coatings obtained by electrochemical oxidation, both for single nanotube layers (EO) and for double layers (TO + EO), similar roughness values were obtained, which were only slightly higher than for the polished material. The highest roughness parameters were observed for samples after thermal oxidation.

Based on the literature [66,67] various structures can be observed in the XRD charts (Fig. 5). For each sample, and in particular, for the substrate alloy, specific reflexes at certain angles are seen. For samples made of Ti-13Nb-13Zr alloy (Fig. 5a) subjected to grinding and polishing

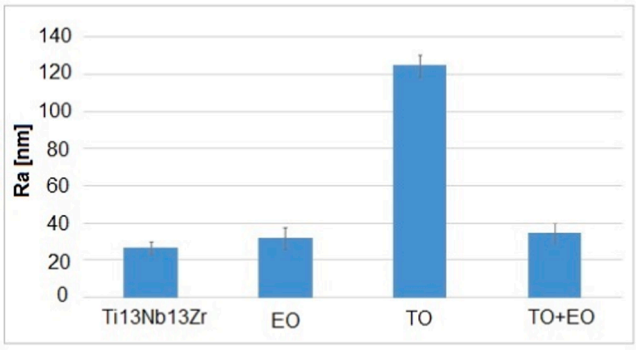

Fig. 4. Roughness (R_a) measured in the area of 200 × 200 nm.

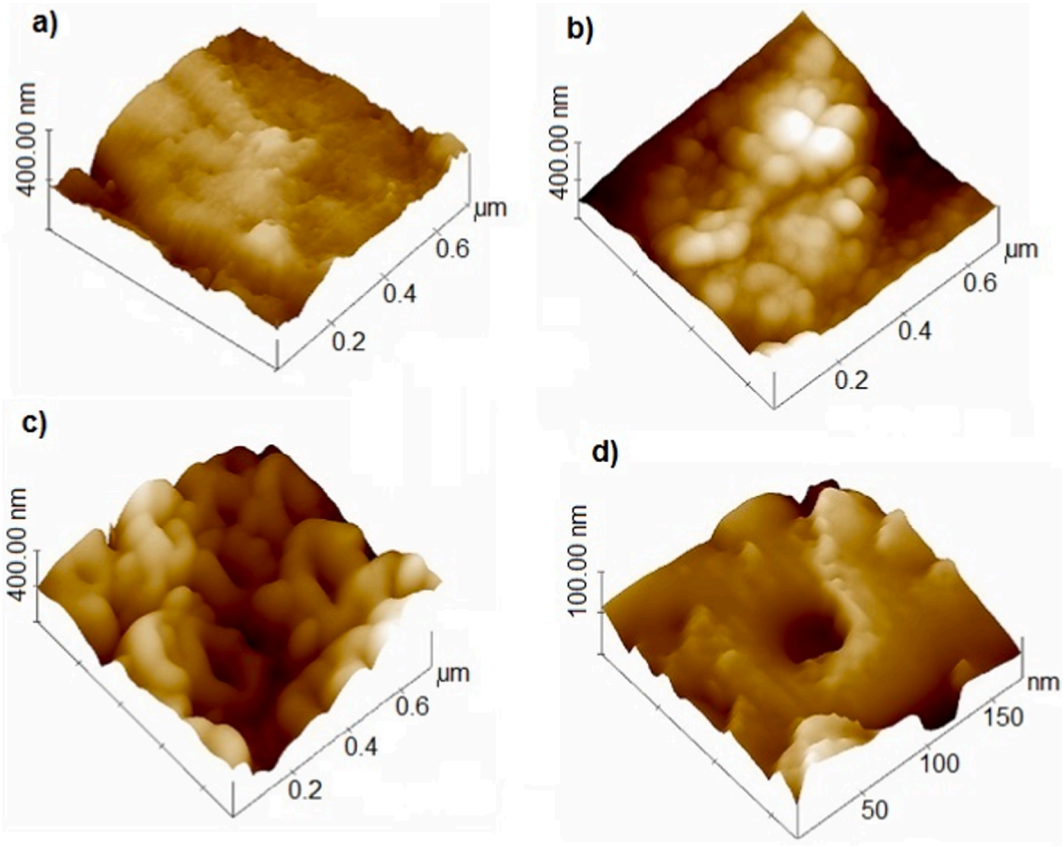

Fig. 3. The surface topography of AFM images for (a) Ti13Nb13Zr alloy, (b) alloy after TO treatment, (c) alloy after TO + EO treatment, (d) a single nanotube.

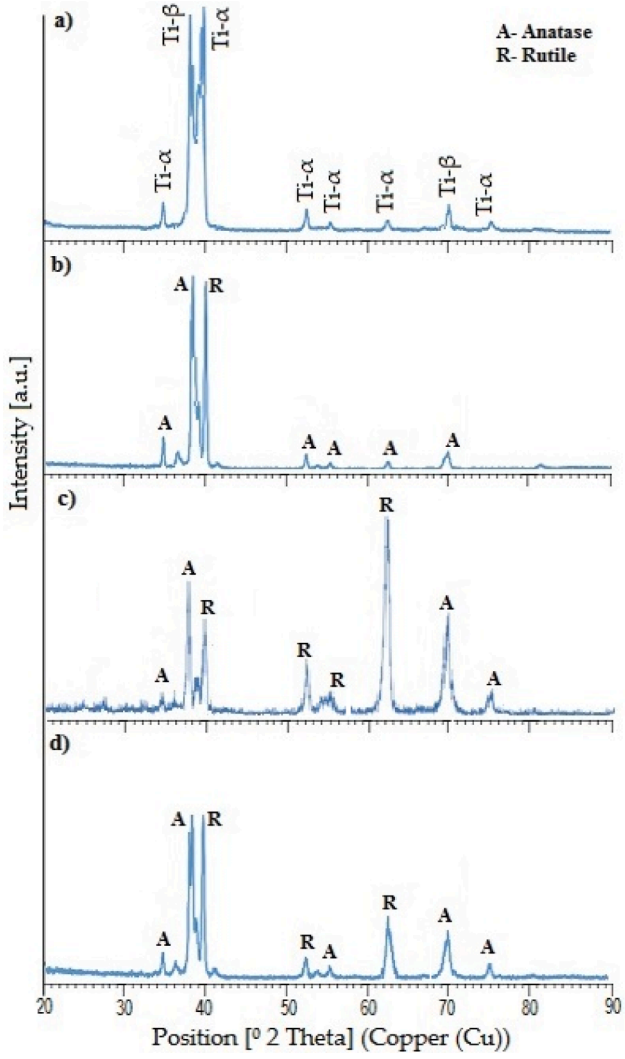

Fig. 5. XRD spectrum for (a) substrate titanium alloy, (b) EO, (c) TO, (d) TO + EO.

processes (without heat treatment processes), characteristic reflections are corresponding to the α -Ti and β-Ti phase positions. On the surface of the samples with produced surface layers (EO, TO, TO + EO), on which the heat treatment processes (annealing - EO, TO + EO) were carried out, there are anatase and rutile structures. The intensity and width of the peaks depend on the size of the crystallites. Depending on the produced layers and carried out heat treatment process (especially the process temperature), the samples differ in the content of individual crystal structures. The EO layers (Fig. 5b) contained mainly anatase, while the TO layers (Fig. 5c) were dominated by rutile. The TO + EO layers have been expected, similarly to the EO (Fig. 5b), to possess the dominant anatase content. However, the research shows that a rutile content is higher than for EO, and the intensity of the main anatase peak is also higher. The intensity of the rutile peaks is however lower compared to TO.

Raman spectroscopy (RS) [68] is a non-invasive test method that allows determining the degree of crystallinity and the quality of the material. Thanks to this technique, it is possible to identify the crystalline phases which make up TiO_2 [69]. In the Raman spectrum (Fig. 6), appropriate modes A_{1g}, B_{2g}, E_g are used, which cause symmetrical bending vibrations (A_{1g}), symmetrical bending vibrations (B_{2g}), and symmetrical stretching vibrations (E_g) [70]. Using this technique, sharp 144 cm^{-1} anatase-derived peaks associated with E_g bundles and 519 cm^{-1} associated with A_{1g}, B_{1g} bundles were identified in the Raman

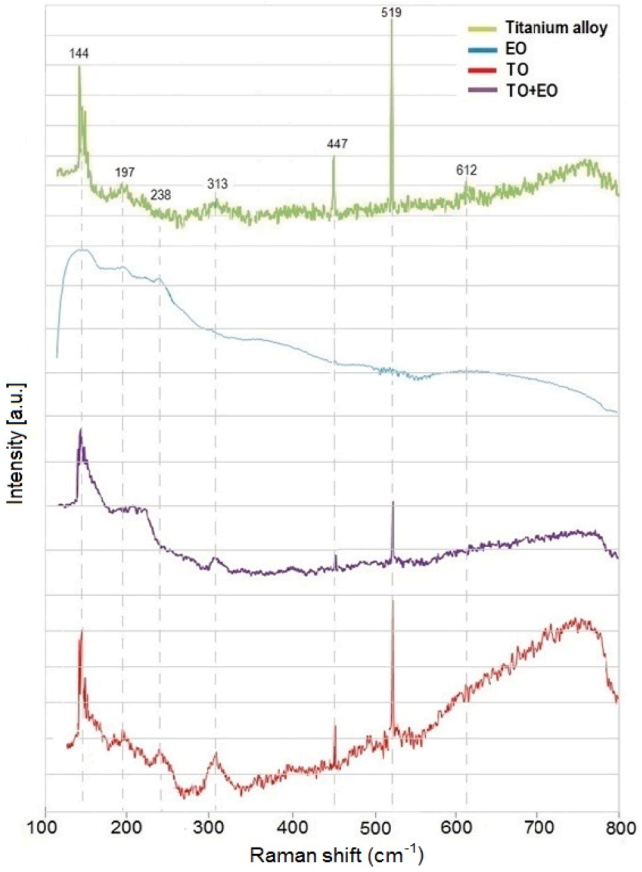

Fig. 6. Raman spectra of the oxide coatings.

spectra. There were also sharp peaks of 447 cm^{-1}, 612 cm^{-1} associated with the vibration modes B_{2g} and A_{1g} beams, characterizing the rutile phase respectively. The anatase phase was also identified by the XRD diffraction peaks. The intensity of the diffraction peak increased with rising temperature [71], as seen in the TO plot.

The dimensions of the crystallites present in the layer are important. It is generally known that when dealing with small crystallites, phonon propagation describes a finite correlation length with dimensions of the same order as the dimensions of crystallites and the relaxation of the selection rule for phonon shoots [71]. In contrast, the smaller the crystallized dimensions, the wider (and more energetic) the peak.

Fig. 7 presents the mechanical properties of the specimens - Young's modulus and hardness. The load-to-displacement curves and nanoindentation measurements illustrate the effects of the different coatings on the mechanical behavior of a surface. TO layers had a crystalline structure and therefore they possessed much higher hardness than the layers obtained by EO. The nanotubular structure had the lowest hardness typical of a layer composed of long thin nanotubes. However, for the TO + EO coating, the hardness values were intermediate between the EO and TO layers. An important factor affecting the measurement of the hardness value, which may cause errors in nanoindentation tests, is the thickness of the oxide layer [72–74]. It is known that the indentation depends on the response of the substrate and the subsequent surface layers [75]. Maximum indent depths were here well below the total thicknesses of the measured layers, and no response from the substrate could be expected.

Fig. 8 illustrates the results of the GDOES measurements. The values of wavelengths emitted by the excitation of atoms appeared for all present elements. For the titanium alloy (Fig. 8a), the distribution of elements with erosion (sputtering) time was abrupt and remained at a certain level.

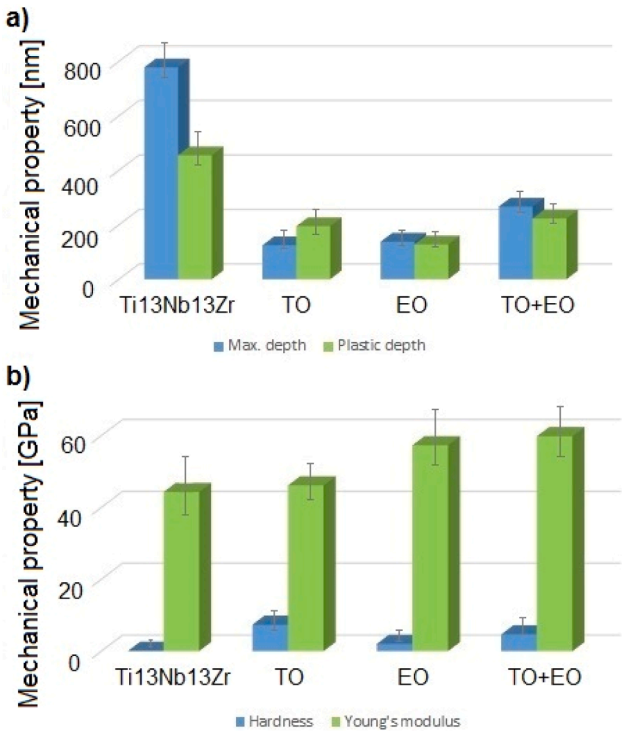

Fig. 7. Nanoindentation test results. Mechanical property: (a) maximal depth and plastic depth, (b) hardness and Young's modulus.

The distribution of the intensity of individual elements for the alloy with the produced layers is different as in the EDX examination. In the case of the EO, TO, and TO + EO coatings, the intensity fluctuations of the alloying elements appeared. In the initial phase of the research, there were clear fluctuations in the intensity of the main alloying elements: Ti, Nb, and Zr. The oxygen content was slightly different for various coatings and the substrate, but for each coating, the highest value was characteristic for the first erosion phase (maxima) that could be identified as resulted from the presence of oxide coatings of different thicknesses.

3.2. Wettability testing

The examined layers differed in the average angle (Fig. 9), which for the Ti-13Nb-13Zr alloy indicated hydrophobic surface, and for the oxide-coated titanium alloy, the hydrophilic surface was observed. For materials intended to come into contact with hard tissue, the contact angle should be between 35° and 80° [62,76]. The TO and TO + EO coatings have wettability within this range.

3.3. Corrosion behavior

The susceptibility to pitting corrosion depends on the type and properties of the material, as well as on the characteristics of the environment. The corrosion resistance of metal alloys was tested in various environments used in implantology. Liu et al. [77] after producing a titanium oxide layer (sol–gel method, thickness of 205 nm) tested the corrosion resistance of a thin film in Tyrode's solution. Pool et al. [78] used blood plasma to test the corrosion resistance of NiTi alloy with titanium dioxide layer modified as a result of ion implantation. Similar research was also carried out in Ringer's solution [79].

Fig. 10 shows the potentiodynamic polarization curves for the

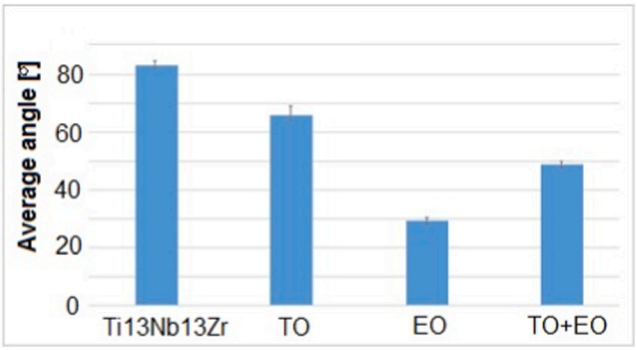

Fig. 9. The average contact angle results.

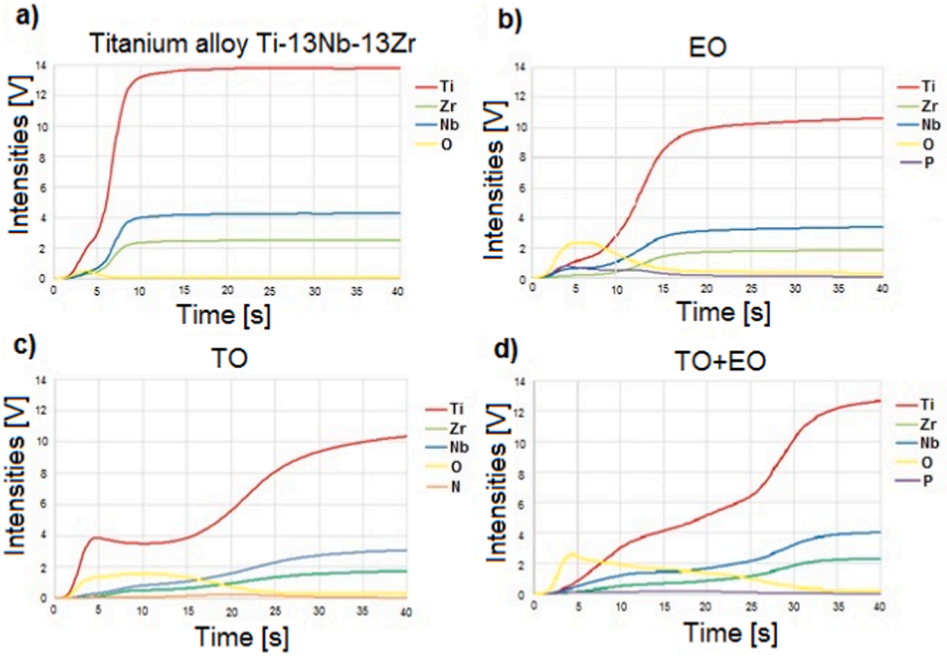

Fig. 8. GDOES analysis results: (a) titanium alloy Ti13Nb13Zr, (b) EO, (c) TO, (d) TO + EO.

polished titanium alloy Ti-13Nb-13Zr, as well as for the produced by electrochemical (EO) and thermal oxidation methods (TO, TO + EO) coatings. As can be seen, not all layers showed good corrosion resistance. The nanotubular oxide layer was characterized by the best protective properties, and very close values were obtained for the reference samples, i.e. titanium alloy subjected to polishing and grinding. The samples with gas-formed layers (TO) turned out to be the most susceptible to the corrosive environment, while the samples covered with TO + EO layers showed higher corrosion resistance compared to TO layers and lower than EO.

The factor proving the improvement of the corrosion resistance is the decrease in the value of the corrosion current density I_{corr} coefficient with the simultaneous increase in the corrosion potential Ecorr.

After analyzing the obtained parameters and the collective characteristics (Table 2), it was noticed that the highest corrosion resistance was demonstrated by the titanium alloy with the applied double layer TO (700 °C) + EO. The analysis of the data on the value of the Ecorr corrosion potential and the corrosion current density I_{corr} showed a slight increase in the corrosion resistance of the TO (700 °C) + EO layers. The corrosion current density for the polished alloy is at least one order of magnitude higher than that of the nanotube layers.

3.4. Biological studies

In cytotoxicity tests (Fig. 11), the five-day-old cultures formed a relatively even layer of cells (monolayers), with a large number of mitotic divisions: metaphase and prophase, and a small number of polymorphs (polycarrions) with no signs of cell damage. The cell culture image showed that the examined layers did not change and did not affect the behavior of osteoblasts.

Table 2
Corrosion current density and corrosion potential at pH 7.

Sample	Corrosion Parameters	
	E_{corr} (V)	I_{corr} (μA/cm^2)
Titanium alloy	−1.78	5.16×10^{-8}
EO	− 0.91	$1{,}65 \times 10^{-9}$
TO (700)	−1.45	1.19×10^{-6}
TO (800)	−1.39	4.47×10^{-7}
TO (900)	−0.13	2.71×10^{-7}
TO (700) + EO	−1,50	1.15×10^{-5}

Fig. 12 presents intensities of biofilm formation on the surface of materials, measured by the absorbance values of formazan solutions (diluted in DMSO) produced by live bacterial cells with MTT. After one day's exposure, the lowest absorbance values were observed for the reference samples. The presence of the nanotubular surface markedly accelerated the biofilm formation, which increased significantly after five days. The lowest levels were obtained for the TO samples for which a slight decrease in biofilm formation was observed. In contrast, for samples with a nanotubes layer (EO and TO + EO), only a slight difference was noticed between the first and fifth days.

Nanotube layers are used in medicine for several reasons. Firstly, due to the increase in roughness, compared to the ground, polished surface of titanium alloys, they provide much better adhesion of the hydroxyapatite coating, but also facilitate the adhesion of *S. aureus*, *S. epidermidis*

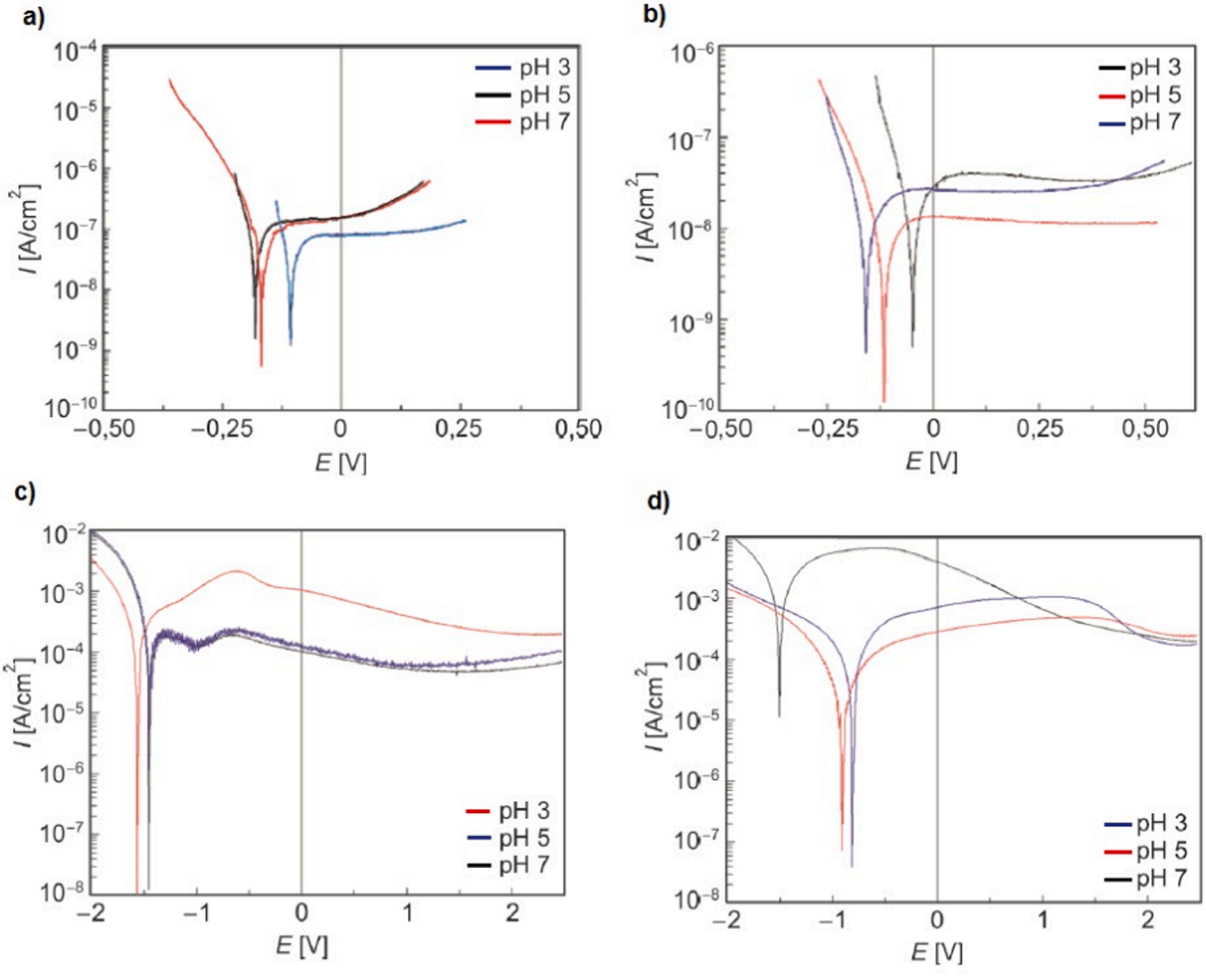

Fig. 10. Measurements of potentiodynamic polarization curves for (a) titanium alloy; (b) EO; (c) TO; (d) TO + EO.

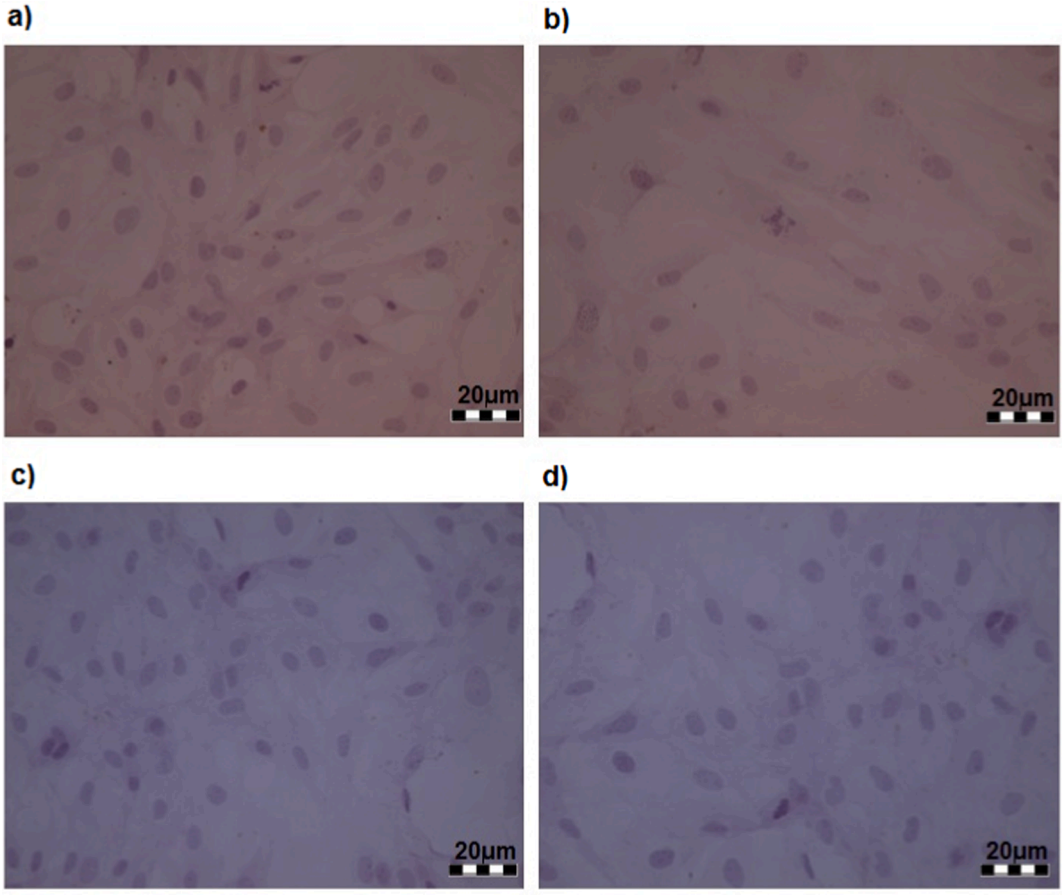

Fig. 11. Cytotoxic tests of osteoblasts cells: (a) titanium alloy; (b) EO; (c) TO; (d) TO + EO.

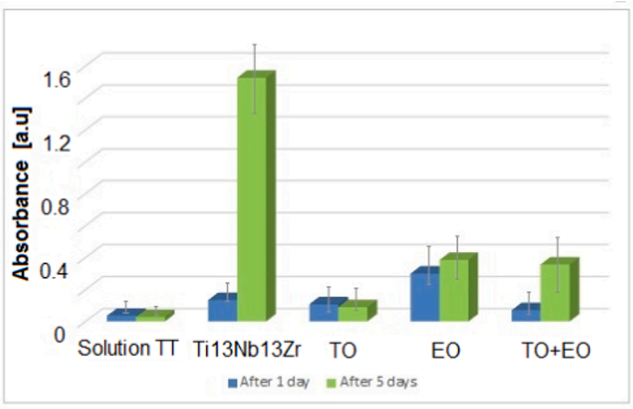

Fig. 12. Test of the bacterial film with used *Staphylococcus aureus*.

[80] and Pseudomonas aeruginosa [81]. The opinions on this subject are divided, Ercan [82] observed a significant reduction of *S. aureus* biofilm formation on nanotube layers after 2 days of cultivation. There are reports on the influence of the chemical composition of nanotube layers, more specifically fluoride ions, on the adhesion of bacteria [81–83].

On the other hand, the number of cells adhering to the surface of nanotubes is greater compared to polished titanium and depends on the diameter of the nanotubes and the phase structure. Lewandowska et al. [84] found that fibroblasts induced on the surface of TiO_2 nanotubes began to form filopodia that penetrated the nanotubes. Secondly, nanotubes, due to their elongated cylindrical shape and significant loading capacity, are attractive for drug delivery systems [85–87], it is possible to contain antibiotics and nanometals providing local protection against microbes. For example, the introduction of vancomecin [88] resulted in a 40% reduction in the spread of *S. aureus*. On the other hand, the use of gentamecin by Lin et al [89] limited the adhesion of *S. aureus*, *S. epidermidis*. The nanotube layer does not increase and sometimes even lowers the corrosion resistance, and thus also the biocompatibility and lifetime of the implant.

4. Discussion

The heat treatment performed here to obtain a change in crystallinity might have a certain effect on the mechanical properties of titanium substrate. However, the increase in grain size is significant for this class of alloys at temperatures over 850 °C [90], far above those here applied. Moreover, for similar Ti6Al4V alloy, annealing at 600 °C for 3 h resulted in improved ductility and strength [91]. Summarizing commonly applied heat treatment of nanotubes used also here is not expected to negatively influence the mechanical properties of the implant.

Compared to the data in the literature [92–94], the achieved results of thermal oxidation of titanium alloys appear similar. However, there were differences in the thickness of the layers, which grew following the mechanisms of the process kinetics [42]. The appearance of anatase and rutile is predicted by the thermodynamics of the formation of oxide phases on titanium in the air. The formation of high surface roughness after oxidation at higher temperatures can be explained by nucleation and the growth of a new phase - rutile. The porosity of the alloy allows for the formation of oxide layers not only on the surface but also inside the pores, at depths that can be tested without the need for cross-sections. Our recent (so far unpublished) data indicate the formation of oxide layers within the pores occurs in the entire volume of the porous

titanium alloy.

An important new observation is a change in the contents of elements in the oxide layers as the temperature increases during TO treatment. This proves a very favorable phenomenon of enriching the layer with zirconium and niobium oxides, with a simultaneous decrease in the amount and fraction of titanium oxide. Presumably, it is the result of the core diffusion of titanium and oxygen, and the spinal diffusion of zirconium and niobium. The increase in roughness promotes both the adhesion of osteoblasts and the possibility of deposition of another oxide, phosphate, and composite coatings on the primary surface of thermally obtained oxide layers. This is particularly important for the development of surface modification technology for screw dental implants.

By applying thermal and electrochemical oxidation, a crystalline nanotubular coating was obtained only on samples oxidized at the lowest temperature, 700 °C. The quite satisfactory protective properties of titanium and its alloys after thermal oxidation, even surprisingly worse than after electrochemical oxidation, are a consequence of the appearance of compact and dense oxide film [95].

The dense, homogeneous nanotubular layers obtained as a result of two-stage oxidation (TO + EO) have different lengths and diameters of nanotubes, similar to one-stage oxidation (EO). That means that there is no significant difference for the growth of oxides either on titanium structure or oxide ceramic crystal phase. However, this process seems more complex as the thickness of the nanotubular layer after TO + EO modification is lower than that after a single EO treatment. It is certainly related to the slower diffusion of oxygen in the previous oxide phase (after TO) than in the alloy structure.

No nanotubular layers were obtained on the samples thermally oxidized at 800 °C and 900 °C. The reason for the lack of the nanotubes is a thick, dense, high resistant inner oxide layer formed as a result of high-temperature thermal oxidation, which prevents the flow of ions between the parent material and the solution.

The GDOES tests carried out show that all the produced layers contain mainly elements such as titanium, zirconium, niobium, and oxygen, as confirmed by previous EDS tests. The lowest oxygen level in the layers was demonstrated for the Ti-13Nb-13Zr alloy, no underwent any additional oxidation (only polished). In such conditions, a layer of titanium oxide with a thickness of only a few nanometers was spontaneously formed. Double layers (TO + EO) showed the highest oxygen content in the layer what could be attributed to the development of the nanotubes into which oxygen can penetrate.

Interesting is also the course of such curves for titanium, as its contents at the surface are quite low, while after, as a result of further atomization, the intensity of titanium increased. However, for the TO samples there was an increase in titanium content, then a temporary decrease, and another increase. On the other side, for TO + EO, a gradual, very moderate increase in the titanium content was observed at a distance from the surface. This may be due to the presence of two layers with a different structure and/or the presence of titanium oxide with a different structure, e.g. non-stoichiometric oxide of the TiO_{2-X} type. The report of Shimizu et al. [96] suggested the atomization rate of the amorphous oxide layer (142 nm thick), formed in sodium chromate solution, as of 15.3 nm/s.

The electrochemical potentiodynamic tests showed that the surface characteristics and thickness of the obtained layers have a significant impact on corrosion resistance. The lowest corrosion resistance after EO oxidation among all treatments, and lower its value after TO + EO modification, compared to TO alone, are visible. It could be easy to explain the lowered corrosion resistance (strictly, corrosion current density) by the presence of nanotubular (or nanocrystalline, in general) structure which possesses a large number of grain boundaries acting as channels for fast atomic diffusion [97,98]. The potential corrosion sites for nanotube layers may be corrosion tunnels, free spaces inside and between the nanotubes. On the other hand, the corrosion resistance in presence of the oxide layer of the nanotubular structure is higher than that of base metal, as already shown [99]. However, the best corrosion resistance for the nanotubular layer may be evidence that corrosion tunnels are not important in corrosion progress, but nanotubes formed during anodization are distinctly resistant to electrochemical corrosion for reasons so far difficult to understand. The high difference can be attributed to the extraordinary stability of nanostructures, but the exact model of dissolution of nanotubes cannot be given yet for this specific case.

5. Conclusions

The applied technologies of thermal and electrochemical oxidation at appropriate process parameters, as well as their combination in two-stage oxidation, make it possible to obtain double (sandwich) coating on the titanium substrate. As a result of thermal oxidation, an oxide layer with a crystalline structure is formed, consisting of anatase and rutile. On the other hand, the anodizing process carried out in solutions containing fluoride ions results in a protective oxide layer with a bioactive nanotubular oxide surface structure if the previous TO oxide layer is obtained at a temperature of about 700 °C. Two-stage oxidation leads then to the formation of the double coating.

The appearance of the double coating is possible only at some thermal oxidation temperatures. The lower oxidation temperatures may not bring out any significantly thick oxide layer, and the higher temperatures result in the oxide layers constituting the effective barrier for diffusion of elements. The creation of the nanotubular oxide layer may occur by chemical etching of oxide layer and electrochemical oxidation, but the increasing thickness of the oxide ceramic layer formed during thermal treatment increases its resistivity, decreases the current flow, and finally stop the formation of the nanotubes.

The produced titanium oxide crystalline double coatings show high surface roughness, high corrosion resistance, are hydrophilic, slightly antibacterial, and not cytotoxic. Therefore they are expected to have a significant impact on an enhancement of the implant-bone integration process, the process of bone tissue growth, and an improved lifetime of the titanium implants.

Titanium oxide nanotube arrays have been proposed for different medical applications, among others in nanotheraupetics by filling nanotubes with enzymes and proteins, with active or immunosuppressive agents, and antibacterial antibiotics or nanometals [100,101]. This research has a potential for the development of such nanostructures on titanium implants as shown innovative technology leaves biocompatibility and bioactivity of so far nanotubular layers, while strengthening corrosion resistance and in such a way enlarging lifetime of implants.

CRediT authorship contribution statement

Agnieszka Ossowska: Conceptualization, Methodology, Validation, Investigation, Resources, Writing - original draft, Writing - review & editing. **Jean-Marc Olive:** Methodology, Validation, Investigation, Resources. **Andrzej Zieliński:** Formal analysis, Writing - review & editing. **Andrzej Wojtowicz:** Methodology.

Declaration of Competing Interest

The authors declare that they have no known competing financial interests or personal relationships that could have appeared to influence the work reported in this paper.

Acknowledgments

We are grateful to Prof. Maria Gazda (Gdansk Techn.) for the research with XRD, Dr. Grzegorz Gajowiec (Gdansk Techn.) for his examinations of oxidized surfaces with the SEM and EDS, the research staff of the Institut de Mécanique et d'Ingénierie de Bordeaux for the AFM and GDOES tests, Prof. Dieter Scharnweber and his group from the Max-

Bergmann-Centrum of Biomaterials, Dresden Technical University for Raman spectroscopy and Prof. Piotr Szweda (Gdansk Techn.) for carrying out antibacterials research.

References

[1] S. Konovalov, I. Komissarova, Y. Ivanov, V. Gromov, D. Kosinov, Structural and phase changes under electropulse treatment of fatigue-loaded titanium alloy VT1-0, J. Mater Res Technol. 8 (1) (2019) 1300–1307, https://doi.org/10.1016/j.jmrt.2018.09.008.

[2] M. Niinomi, M. Nakai, J. Hieda, Development of new metallic alloys for biomedical applications, Acta Biomater. 8 (2012) 3888–3903, https://doi.org/10.1016/j.actbio.2012.06.037.

[3] A. Alsaran, G. Purcek, I. Hacisalihoglu, Y. Vangolu, O. Bayrak, I. Karaman, A. Celik, Hydroxyapatite production on ultrafine-grained pure titanium by micro-arc o.xidation and hydrothermal treatment, Surf. Coat. Technol. 205 (2011) S537–S542. https://doi:10.1016/j.surfcoat.2011.03.032.

[4] K.C. Kung, T.M. Lee, T.S. Lui, Bioactivity and corrosion properties of novel coatings containing strontium by micro-arc oxidation, J. Alloys Compd. 508 (2) (2010) 384–390, https://doi.org/10.1016/j.jallcom.2010.08.057.

[5] L. Xie, C. Liu, Y. Song, H. Guo, Z. Wang, L. Hua, L. Wang, L.-C. Zhang, Evaluation of microstructure variation of TC11 alloy after electroshocking treatment, J. Mater. Res. Technol. 9 (2) (2020) 2455–2466, https://doi.org/10.1016/j.jmrt.2019.12.076.

[6] Y.F. Jia, R.J. Pan, P.Y. Zhang, Z.T. Sun, X.R. Chen, X.C. Zhang, X.J. Wu, Enhanced surface strengthening of titanium treated by combined surface deep-rolling and oxygen boost diffusion technique, Corros. Sci. 157 (2019) 256–267, https://doi.org/10.1016/j.corsci.2019.05.020.

[7] D. Banerjee, J.C. Williams, Perspectives on titanium science and technology, Acta Mater. 61 (2013) 844–879, https://doi.org/10.1016/j.actamat.2012.10.043.

[8] P. Ducheyne, Q. Qiu, Bioactive ceramics: the effect of surface reactivity on bone formation and bone cell function, Biomaterials 20 (23–24) (1999) 2287–2303, https://doi.org/10.1016/S0142-9612(99)00181-7.

[9] A. Bartkowiak, A. Zarzycki, S. Kac, M. Perzanowski, M. Marszalek, Mechanical properties of different nanopatterned TiO_2 substrates and their effect on hydrothermally synthesized bioactive hydroxyapatite coatings, Materials 13 (22) (2020) 5290, https://doi.org/10.3390/ma13225290.

[10] F. Suska, L. Emanuelsson, A. Johansson, P. Tengvall, P. Thomsen, Fibrous capsule formation around titanium and copper, J. Biomed. Mater. Res. Part A 85 (2008) 888–896, https://doi.org/10.1002/jbm.a.31575.

[11] H.C.H. Ko, B.K. Milthorpe, C.D. McFarland, Engineering Thick Tissues – The Vascularisation Problem, Eur. Cells Mater. 14 (2007) 1–19, https://doi.org/10.22203/ecm.v014a01.

[12] D. Krupa, J. Baszkiewicz, J. Sobczak, A. Biliński, A. Barcz, Modifying the properties of titanium surface with the aim of improving its bioactivity and corrosion resistance, J. Mater. Process Technol. 143–144 (2003) 158–163, https://doi.org/10.1016/S0924-0136(03)00398-4.

[13] M.S. Sader, I.S. Bastos, G.A. Soaresde, Improvement of in vitro titanium bioactivity by three different surface treatments, Dent. Mater. 22 (3) (2006) 275–282. https://doi.org/10.1016/j.dental.2005.03.012.

[14] J.E. Lemons, Biomaterials, Biomechanics, Tissue Healing, and Immediate-Function Dental Implants, J. Oral Implantol. 30 (2004) 318–324, https://doi.org/10.1563/0712.1.

[15] S. Izman, M.R.A. Kadir, M. Anwar, E.M. Nazim, R. Rosliza, E.M. Abdullah, M.A. Hassan, Surface modification techniques for biomedical grade of titanium alloys: oxidation, carburization and ion implantation processes, in Titanium Alloys - Towards Achieving Enhanced Properties, for Diversified Applications 9 (2012) 201–228. doi:10.5772/36318.

[16] P. Maurel, L. Weiss, P. Bocher, E. Fleury, T. Grosdidier, Oxide dependent wear mechanisms of titanium against a steel counterface: Influence of SMAT nanostructured surface, Wear 430–431 (2019) 245–255, https://doi.org/10.1016/j.wear.2019.203087.

[17] R. Huang, L. Zhang, L. Huang, J. Zhu, Enhanced in-vitro osteoblastic functions on _-type titanium alloy using surface mechanical attrition treatment, Mater. Sci. Eng. C 97 (2019) 688–697, https://doi.org/10.1016/j.msec.2018.12.082.

[18] P. Ghensi, E. Bressan, C. Gardin, L. Ferroni, L. Ruffato, M. Caberlotto, C. Soldini, B. Zavan, Osteogrowth induction titanium surface treatment reduces ROS production of mesenchymal stem cells increasing their osteogenic commitment, Mater. Sci. Eng. C 74 (2017) 389–398, https://doi.org/10.1016/j.msec.2016.12.032.

[19] M. Parchanska-Kowalik, E. Wołowiec-Korecka, L. Klimek, Effect of chemical surface treatment of titanium on its bond with dental ceramics, J. Prosthet. Dent. 120 (2018) 470–475.

[20] W.S.W. Harun, R.I.M. Asri, J. Alias, F.H. Zulkifli, K. Kadirgama, S.A.C. Ghani, J.H.M. Shariffuddin, A comprehensive review of hydroxyapatite-based coatings adhesion on metallic biomaterials, Ceram. Int. 44 (2018) 1250–1268. https://doi.org/10.1016/j.ceramint.2017.10.162.

[21] M. Supernak-Marczewska, A. Ossowska, P. Strakowska, A. Zielinski, Nanotubular oxide layers and hydroxyapatite coatings on porous titanium alloy Ti13Nb13Zr, Adv. Mater. Sci. 18 (2018) 17–23, https://doi.org/10.1515/adms-2017-0046.

[22] D. Li, K. Li, H. Shan, Improving biocompatibility of titanium alloy scafolds by calcium incorporated silicalite-1 coatings, Inorg. Chem. Commun. 102 (2019) 61–65, https://doi.org/10.1016/j.inoche.2019.02.004.

[23] N. Karimi, M. Kharaziha, K. Raeissi, Electrophoretic deposition of chitosan reinforced graphene oxide-hydroxyapatite on the anodized titanium to improve biological and electrochemical characteristics, Mater. Sci. Eng. C 98 (2019) 140–152, https://doi.org/10.1016/j.msec.2018.12.136.

[24] L. Fathyunes, J. Khalil-Allafi, M. Moosavifar, Development of graphene oxide/calcium phosphate coating by pulse electrodeposition on anodized titanium: Biocorrosion and mechanical behavior, J. Mech. Behav. Biomed. Mater. 90 (2019) 575–586, https://doi.org/10.1016/j.jmbbm.2018.11.011.

[25] S. Franz, D. Perego, O. Marchese, A. Lucotti, M. Bestetti, Photoactive TiO_2 coatings obtained by plasma electrolytic oxidation in refrigerated electrolytes, Appl. Surf. Sci. 385 (2016) 498–505, https://doi.org/10.1016/j.apsusc.2016.05.032.

[26] D.N. Gopala Krishna, R.P. George, J. Philip, Determination of nanoscale titanium oxide thin film phase composition using X-ray photoelectron spectroscopy valence band analysis, Thin Solid Films 681 (2019) 58–68, https://doi.org/10.1016/j.tsf.2019.04.044.

[27] Y. Liu, X. Chen, Black titanium dioxide for photocatalysis, Semiconduct. Semimet. 97 (2017) 393–428, https://doi.org/10.1016/bs.semsem.2017.04.001.

[28] C. Croitoru, I.C. Roata, A. Pascu, E.M. Stanciu, I. Hulka, G. Stoian, N. Lupu, Photocatalytic surfaces obtained through one-step thermal spraying of titanium, Appl. Surf. Sci. 504 (2020), 144173, https://doi.org/10.1016/j.apsusc.2019.144173.

[29] G.L. Lin, K.D. Hankenson, Integration of BMP, Wnt, and notch signaling pathways in osteoblast differentiation, J. Cell. Biochem 112 (12) (2011) 3491–3501, https://doi.org/10.1002/jcb.23287.

[30] C. Nicolaije, M. Koedam, J.P.T.M. van Leeuwen, Decreased oxygen tension lowers reactive oxygen species and apoptosis and inhibits osteoblast matrix mineralization through changes in early osteoblast differentiation, J. Cell Physiol 227 (4) (2012) 1309–1318, https://doi.org/10.1002/jcp.22841.

[31] T. Kokubo, Design of bioactive bone substitutes based on biomineralization process, Mater. Sci. Eng. C 25 (2005) 97–104, https://doi:10.1016/j.msec.2005.01.002.

[32] C. Von Wilmowsky, S. Bauer, R. Lutz, M. Meisel, F.W. Neukam, T. Toyoshima, P. Schmuki, E. Nkenke, K.A. Schlegel, In Vivo Evaluation of Anodic TiO_2 Nanotubes, An Experimental Study in the Pig, J. Biomed. Mater. Res. Part B Appl. Biomater. 89 (2009) 165–171, https://doi.org/10.1002/jbm.b.31201.

[33] C. Xie, Bio-inspired nanofunctionalization of biomaterial surface: a review, Biosurface and Biotribology 5 (3) (2019) 83–92, https://doi.org/10.1049/bsbt.2019.0009.

[34] P. Santiago-Medina, P.A. Sundaram, N. Diffoot-Carlo, The effects of micro arc oxidation of gamma titanium aluminide surfaces on osteoblast adhesion and differentiation, J Mater Sci Mater Med 25 (6) (2014) 1577–1587, https://doi.org/10.1007/s10856-014-5179-3.

[35] A. Ossowska, S. Sobieszczyk, M. Supernak, A. Zieliński, Morphology and properties of nanotubular oxide layer on the Ti13Zr13Nb alloy, Surf. Coat. Technol. 258 (2014) 1239–1248, https://doi.org/10.1016/j.surfcoat.2014.06.054.

[36] A. Ossowska, A. Zieliński, M. Supernak, Electrochemical oxidation and corrosion resistance of the Ti13Nb13Zr alloy, Biomaterials, XVI (122-123) (2013) 4-6. http://yadda.icm.edu.pl/yadda/element/bwmeta1.element.baztech-818f0ea0-1df0-4fe2-9af9-4033012c1da1 (accessed 10 November 2013).

[37] D.S. Rama Krishna, Y.L. Brama, Y. Sun, Tick rutile layer on titanium for tribological applications, Tribol Int. 40 (2007) 329–334, https://doi.org/10.1016/j.triboint.2005.08.004.

[38] O. Yamamoto, K. Alvarez, T. Kikuchi, Z. Fukuda, Fabrication and characterization of oxygen-diffused titanium for biomedical applications, Acta Biomat. 5 (2009) 3605–3615, https://doi.org/10.1016/j.actbio.2009.06.011.

[39] R. Bansal, J.K. Singh, V. Singh, D.D.N. Singh, P. Das, Optimization of oxidation temperature for commercially pure titanium to achieve improved corrosion resistance, J. Mater. Eng. Perform. 26 (9) (2017) 69–977, https://doi.org/10.1007/s11665-017-2515-z.

[40] R. Ding, W. Li, X. Wang, T. Gui, B. Li, P. Han, H. Tian, A. Liu, X. Wang, X. Liu, X. Gao, W. Wang, L. Song, A brief review of corrosion protective films and coatings based on graphene and graphene oxide, J. Alloy. Compd. 764 (2018) 1039–1055, https://doi.org/10.1016/j.jallcom.2018.06.133.

[41] Z. Qi, Z. Wu, D. Zhang, J. Zuo, Z. Wang, Microstructure, mechanical properties and oxidation behaviors of magnetron sputtered NbN_x coatings, J. Alloy. Compd. 675 (2016) 22–30, https://doi.org/10.1016/j.jallcom.2016.03.109.

[42] J. Dai, J. Zhu, C. Chen, F. Weng, High temperature oxidation behavior and research status of modifications on improving high tempreture oxidation resistance of titanium alloy ant titanium aluminides: A review, J. of Alloys and Compounds 685 (2016) 784–798, https://doi.org/10.1016/j.jallcom.2016.06.212.

[43] C.A.R. Maestro, A.H.S. Bueno, A.M. de Sousa Malafaia, Cyclic thermal oxidation evaluation to improve Ti6Al4V surface in applications as biomaterial, J. Mater. Eng. Perform. 28 (8) (2019) 4991–4997. https://doi.org/10.1007/s11665-019-04220-x.

[44] S. Wang, Y. Liu, C. Zhang, Z. Liao, W. Liu, The improvement of wettability, biotribological behavior and corrosion resistance of titanium alloy pretreated by thermal oxidation, Tribol. Int. 79 (2014) 174–182, https://doi.org/10.1016/j.triboint.2014.06.008.

[45] M.T. Mohammed, Development of surface structure and characteristics of thermally oxidized β-Ti alloy for biomedical applications, Mater. Res. Express 6 (10) (2019), 106589, https://doi.org/10.1088/2053-1591/ab3d98.

[46] Q. Liu, S. Hui, K. Tong, Y. Yu, W. Ye, S. Song, Investigation of high temperature behavior and processing map of Ti-6Al-4V-0.11Ru titanium alloy, J. of Alloys and

Compounds 787 (2019) 527–536, https://doi.org/10.1016/j.jallcom.2019.02.046.
[47] M. Berthaud, I. Popa, R. Chassagnon, O. Heintz, J. Lavkova, S. Chevalier, Study of titanium alloy Ti6242S oxidation behaviour in air at 560°C: Effect of oxygen dissolution on lattice parameters, Corros. Sci. 164 (2020), 108049, https://doi.org/10.1016/j.corsci.2019.06.004.
[48] C. Dupressoire, A. Rouaix-Vande Put, P. Emile, C. Archambeau-Mirguet, R. Peraldi, D. Monceau, Effect of nitrogen on the kinetics of oxide scale growth and of oxygen dissolution in the Ti6242S titanium-based alloy, Oxid. Met. 87 (2017) 343–353, https://doi.org/10.1007/s11085-017-9729-1.
[49] K.R.M. Macedo, G.A.C. Oliveira, K.A.B. Pereira, L.C. Mendes, A.S. Araújo, R. J. Cassella, Titanium-zinc polycitrate precursor: Influence of thermal treatment on structural, thermal, optical characteristics of zinc titanates, Mater. Chem. Phys. 236 (2019), 121768, https://doi.org/10.1016/j.matchemphys.2019.121768.
[50] D.J. Putatunda, Singh On the ground state of TiO_2 as predicted by all electron density functional calculations in relation to experiment, Eur. Phys. J. B 90 (11) (2017) 210, https://doi.org/10.1140/epjb/e2017-80476-9.
[51] S. Siol, N. Ott, C. Beall, M. Stiefel, Y. Unotulmazsoy, M. Döbeli, D. Tilley, P. Schmutz, L.P.H. Jeurgens, C. Cancellieri, A combinatorial guide to phase formation and surface passivation of tungsten titanium oxide prepared by thermal oxidation, Acta Mater. 186 (2020) 95–114, https://doi.org/10.1016/j.actamat.2019.12.026.
[52] Y. Wang, C. Wen, P. Hodgson, Y. Li, Biocompatibility of TiO_2 nanotubes with different topographies, J. Biomed. Mater. Res. Part A 102 (2014) 743–751, https://doi.org/10.1002/jbm.a.34738.
[53] F. Hilario, V. Roche, R.P. Nogueira, A.M.J. Junior, Influence of morphology and crystalline structure of TiO2 nanotubes on their electrochemical properties and apatite-forming ability, Electrochim. Acta 245 (2017) 337–349, https://doi.org/10.1016/j.electacta.2017.05.160.
[54] D. Pradhan, A.W. Wren, S.T. Misture, N.P. Mellott, Investigating the structure and biocompatibility of niobium and titanium oxides as coatings for orthopedic metallic implants, Mater. Sci. Eng. C 58 (2016) 918–926, https://doi.org/10.1016/j.msec.2015.09.059.
[55] G. Wanga, Y. Wana, B. Ren, Z. Liu, Bioactivity of micropatterned TiO2 nanotubes fabricated by micro-milling and anodic oxidation, Mater. Sci. Eng. C 95 (2019) 114–121, https://doi.org/10.1016/j.msec.2018.10.068.
[56] J. Park, S. Bauer, P. Schmuki, Nanosize and vitality: TiO2 nanotube diameter directs cell fate, Nano. Lett. 7 (6) (2007) 1686–1691, https://doi.org/10.1021/nl070678d.
[57] G.E. Aninwene, Ch. Yao, T.J. Webster, Enhanced osteoblast adhesion to drug-coated anodized nanotubular titanium surfaces, Int. J. Nanomed 3 (2) (2008) 257–264, https://doi.org/10.2147/ijn.s2552.
[58] L. Zhao, S. Mei, P.K. Chu, Y. Zhang, Z. Wu, The influence of hierarchical hybrid micro/nano-textured titanium surface with titania nanotubes on osteoblast functions, Biomaterials 31 (19) (2010) 5072–5082, https://doi.org/10.1016/j.biomaterials.2010.03.014.
[59] D.M. Brunette, Principles of cell behavior on titanium surfaces and their application to implanted devices, in: W: Brunette D.M. et al. (Eds.): Titanium in Medicine: Material Science, Surface Science, Biological Responses and Medical Applications, Springer, Heidelberg, Berlin, 2001, pp. 485–512. https://www.researchgate.net/profile/Marcus-Textor/publication/224766482_Surface_composition_and_topography_of_titanium_alloy_implants/links/55d4ddc508ae6788fa35273c/Surface-composition-and-topography-of-titanium-alloy-implants.pdf (accessed 15 February 2021).
[60] S. Bauer, A. Pittrof, H. Tsuchiya, P. Schmuki, Size-effects in TiO2 nanotubes: Diameter dependent anatase/rutile stabilization, Electrochem. commun 13 (6) (2011) 538–541, https://doi.org/10.1016/j.elecom.2011.03.003.
[61] Y.N. Xu, M.N. Liu, M.C. Wang, A. Oloyede, J.M. Bell, C. Yan, Nanoindentation study of the mechanical behavior of TiO2 nanotube arrays, J. Appl. Phys. 118 (2015), 145301, https://doi.org/10.1063/1.4932213.
[62] A. Ossowska, A. Zieliński, J. Olive, A. Wojtowicz, P. Szweda, Influence of Two-Stage Anodization on Properties of the Oxide Coatings on the Ti–13Nb–13Zr Alloy, Coatings 10 (8) (2020) 707–727, https://doi.org/10.3390/coatings10080707.
[63] M.F. López, A. Gutierrez, J.A. Jimenez, M. Martinesi, M. Stio, C. Treves, Thermal oxidation of vanadium-free Ti alloys: an X-ray photoelectron spectroscopy study, Mater. Sci. Eng. C 30 (2010) 465–471, https://doi.org/10.1016/j.msec.2010.01.004.
[64] M. Metikos-Hukovic, A. Kwokal, J. Piljac, The influence of niobium and vanadium on passivity of titanium-based implants in physiological solution, Biomaterials 24 (2003) 3765–3775, https://doi.org/10.1016/S0142-9612(03)00252-7.
[65] I. Golvano, I. Garcia, A. Conde, W. Tato, A. Aginagalde, Influence of fluoride content and pH on corrosion and tribocorrosion behavior of Ti13Nb13Zr alloy in oral environment, J Mech Behav Biomed Mater. 49 (2015) 186–196, https://doi.org/10.1016/j.jmbbm.2015.05.008.
[66] D.M. Gordin, T. Gloriant, V. Chane-Pane, D. Busardo, V. Mitran, D. Höche, C. Vasilescu, S.I. Drob, A. Cimpean, Surface characterization and biocompatibility of titanium alloys implanted with nitrogen by Hardion plus technology, J. Mater. Sci-Mater. Med. 23 (2012) 2953–2966. https://doi.org/10.1007/s10856-012-4750-z.
[67] J. Liqiang, S. Xiaojun, X. Baifu, W. Baiqi, C. Weimin, F. Honggang, The preparation and characterization of La doped TiO2 nanoparticles and their photocatalytic activity, J. Solid State Chem. 177 (10) (2004) 3375–3382, https://doi.org/10.1016/j.jssc.2004.05.064.
[68] J.C. Parker, R.W. Siegel, Raman microprobe study of nanophase TiO2 and oxidation-induced spectral changes, J. Mater. Res. 5 (2011) 1246–1252, https://doi.org/10.1557/JMR.1990.1246.
[69] C.A. Chen, Y.S. Huang, W.H. Chung, D.S. Tsai, K.K. Tiong, Raman spectroscopy study of the phase transformation on nanocrystalline titania films prepared via metal organic vapour deposition, J. Mater. Sci. Mater. Electron. 20 (2009) 303–306, https://doi.org/10.1007/s10854-008-9595-3.
[70] J. Yan, G. Wu, N. Guan, L. Li, Z. Li, X. Cao, Understanding the effect ofsurface/bulk defects on the photocatalytic activity of TiO_2: anatase versusrutile, Phys. Chem. Chem. Phys. 15 (2013) 10978–10988, https://doi.org/10.1039/c3cp50927c.
[71] J.M. Chaves, A.L.A. Escada, A.D. Rodrigues, A.P.R. Alves Claro, Characterization of the structure, thermal stability and wettabilityof the TiO2 nanotubes growth on the Ti–7.5Mo alloy surface, Appl. Surf. Sci. 370 (2016) 76–82, https://doi.org/10.1016/j.apsusc.2016.02.017.
[72] T. Hryniewicz, K. Rokosz, J. Valíček, R. Rokicki, Effect of magnetoelectropolishing on nanohardness and Young's modulus of titanium biomaterial, Mater. Lett. 83 (2012) 69–72, https://doi.org/10.1016/j.matlet.2012.06.010.
[73] A.C. Ficher-Cripps, Critical Review of Analysis and Interpretation of nanoindentation test data, Surf. Coat. Technol. 200 (2006) 4153–4165, https://doi.org/10.1016/j.surfcoat.2005.03.018.
[74] J.R. Tuck, A.M. Korsunsky, D.G. Bhat, S.J. Bull, Indentation hardness evaluation of cathodic arc deposited thin hard coatings. Surf. Coat. Technol. 139 (2001) 63-74. http://nanoproductengineering.com/papers/34.pdf (accessed 8 January 2021).
[75] E. Jiménez-Piquéa, Y. Gaillardb, M. Anglada, Instrumented indentation of layered ceramic materials, Key Eng. Mater. 333 (2007) 107–116, https://doi.org/10.4028/www.scientific.net/KEM.333.107.
[76] J.K. Hirvonen, Ion Implantation, Reference to a chapter in an edited book: Materials -Effect of radiation on, Academic Press, New York, 1980.
[77] J.X. Liu, D.Z. Yang, F. Shi, Y.-J. Cai, Sol–gel deposited TiO_2 film on NiTi surgical alloy for biocompatibility improvement, Thin Solid Films 429 (1–2) (2003) 225–230, https://doi.org/10.1016/S0040-6090(03)00146-9.
[78] R.W.Y. Poon, J.P.Y. Ho, X. Liu, C.Y. Chunga, P.K. Chua, K.W.K. Yeungb, W. W. Lub, K.M.C. Cheungb, Anti-corrosion performance of oxidized and oxygen plasma-implanted NiTi alloys, Mater. Sci. Eng. A 390 (1–2) (2005) 444–451, https://doi.org/10.1016/j.msea.2004.08.061.
[79] A. Ossowska, R. Beutner, D. Scharnweber, A. Zieliński, Properties of Composite Oxide Layers on The Ti13Nb13Zr Alloy, Surf. Eng. 33 (11) (2017) 841–848, https://doi.org/10.1080/02670844.2017.1305657.
[80] B. Ercan, E. Taylor, E. Alpaslan, T.J. Webster, Diameter of titanium nanotubes influences anti-bacterial efficacy, Nanotechnology 22 (29) (2011), 295102 https://doi:10.1088/0957-4484/22/29/295102.
[81] S.D. Puckett, E. Taylor, T. Raimondo, T.J. Webster, The relationship between the nanostructure of titanium surfaces and bacterial attachment, Biomaterials 31 (4) (2010) 706–713, https://doi:10.1016/j.biomaterials.2009.09.081.
[82] B. Ercan, K.M. Kummer, K.M. Tarquinio, T.J. Webster, Decreased Staphylococcus aureus biofilm growth on anodized nanotubular titanium and the effect of electrical stimulation, Acta Biomat. 7 (2011) 3003–3012, https://doi:10.1016/j.actbio.2011.04.002.
[83] E.P. Ivanova, V.K. Truong, J.Y. Wang, C.C. Berndt, R.T. Jones, I.I. Yusuf, Impact of nanoscale roughness of titanium thin film surfaces on bacterial retention, Langmuir. 26 (2010) 1973–1982, https://doi:10.1021/la902623c.
[84] Z. Lewandowska, P. Piszczek, A. Radtke, T. Jedrzejewski, W. Kozak, B. Sadowska, The evaluation of the impact of titania nanotube covers morphology and crystal phase on their biological properties, J Mater Sci: Mater Med 26 (2015) 163, https://doi.org/10.1007/s10856-015-5495-2.
[85] M. Hasanzadeh Kafshgari, D. Kah, A. Mazare, N.T. Nguyen, M. Distaso, W. Peukert, W.H. Goldmann, P. Schmuki, B. Fabry, Anodic titanium dioxidenanotubes for magnetically guided therapeutic delivery, SciRep 9 (2019) 13439, https://doi.org/10.1038/s41598-019-49513-2.
[86] Q. Wang, J.Y. Huang, H.Q. Li, Z. Chen, A.Z. Zhao, Y. Wang, K.Q. Zhang, H.T. Sun, S.S. Al-Deyab, Y.K. Lai, TiO_2 nanotube platforms for smart drug delivery: a review.Int, J. Nanomed. 11 (2016) 4819–4834. https://doi:10.2147/IJN.S108847.
[87] Z.F. Yin, L. Wu, H.G. Yang, Y.H. Su, Recent progress in biomedical applications of titanium dioxide, Phys Chem Chem Phys 15 (2013) 4844–4858, https://doi:10.1039/c3cp43938k.
[88] H. Zhang, Y. Sun, A. Tian, X. Xin Xue, L. Wang, A. Alquhali, X. Bai, Improved antibacterial activity and biocompatibility on vancomycin-loaded TiO2 nanotubes: in vivo and in vitro studies. Int, J Nanomed. 8 (2013) 4379–4389, https://doi.org/10.2147/IJN.S53221.
[89] W. Lin, H. Tan, Z. Duan, B. Yue, R. Ma, G. He, T. Tang, Inhibited bacterial biofilm formation and improved osteogenic activity on gentamicin-loaded titania nanotubes with various diameters, Biomed Microdevices. 16 (2014) 449–458, https://doi.org/10.2147/IJN.S57875, https://.
[90] N. Yumak, K. Aslantas, A Review on heat treatment efficiency in metastable β titanium alloys: the role of treatment process and parameters, J. Mater. Res. Technol. 9 (2020) 15360–15380, https://doi.org/10.1016/j.jmrt.2020.10.088.
[91] J. Sarma, R. Kumar, A.K. Sahoo, A. Panda, Enhancement of materials properties of titanium through heat treatment process: A brief review, Mater. Today: Proceedings 23 (3) (2020) 561–564, https://doi.org/10.1016/j.matpr.2019.05.409.

[92] A. Ashrafizadeh, F. Ashrafizadeh, Structural features and corrosion analysis of thermally oxidized titanium, J. Alloys Compd. 480 (2) (2009) 849–852, https://doi.org/10.1016/j.jallcom.2009.02.079.
[93] A.R. Ebrahimi, F. Zarei, R.A. Khosroshahi, Effect of thermal oxidation process on fatigue behavior of Ti-4Al-2V alloy, Surf. Coat. Technol. 203 (3–4) (2008) 199–203. https://doi.org/10.1016/j.surfcoat.2008.08.038.
[94] S. Kumar, T.S.N. Sankara Narayanan, S.G. Sundara Raman, S.K. Seshadri, Thermal oxidation of Ti6Al4V alloy: microstructural and electrochemical Characterization, Mater. Chem. Phys. 119 (2010) 337–346, https://doi.org/10.1016/j.matchemphys.2009.09.007.
[95] D.V. Mashtalyar, K.V. Nadaraia, I.M. Imshinetskiy, E.A. Belov, V.S. Filonina, S. N. Suchkov, S.L. Sinebryukhov, S.V. Gnedenkov, Composite coatings formed on Ti by POE and fluoropolymer treatment, Appl. Surf. Sci. 536 (2021), 147976, https://doi.org/10.1016/j.apsusc.2020.147976.
[96] K. Shimizu, R. Payling, H. Habazaki, P. Skeldond, G.E. Thompson, Rf-GDOES depth profiling analysis of a monolayer of thiourea adsorbed on copper, J. Anal. At. Spectrom. 19 (2004) 692–695, https://doi.org/10.1039/B400918P.
[97] W.P. Tong, N.R. Tao, Z.B. Wang, J. Lu, K. Lu, Nitriding iron at lower temperatures, Science 299 (2003) 686–688, https://doi.org/10.1126/science.1080216.
[98] Wang Z.B., Tao N.R., Tong W.P., Lu J., Lu K., Diffusion of chromium in nanocrystalline iron produced by means of surface mechanical attrition treatment, Acta Mater. 51 (2003) 4319–4329, https://doi.org/10.1016/S1359-6454(03)00260-X.
[99] V.S. Saji, H.Ch. Choe, W.A. Brantley, An electrochemical study on self-ordered nanoporous and nanotubular oxide on Ti-35Nb-5Ta-7Zr alloy for biomedical applications, Acta Biomater. 5 (6) (2009) 2303–2310, https://doi.org/10.1016/j.actbio.2009.02.017.
[100] A.W. Tan, B. Pingguan-Murphy, R. Ahmad, S.A. Akbar, Review of titania nanotubes: Fabrication and cellular response, Ceram. Int. 38 (2012) 4421–4435, https://doi.org/10.1016/j.ceramint.2012.03.002.
[101] R.B.S.M.N. Mydin, R. Hazan, M.F.F. Wajidi, S. Sreekantan, Titanium Dioxide Nanotube Arrays for Biomedical Implant Materials and Nanomedicine Applications. In Titanium Dioxide - Material for a Sustainable Environment; Editor Yang, D.; IntechOpen, 2018, 469-483. https://doi.org/10.5772/intechopen.73060.